

Application of combined Raman spectroscopy and Electron Probe Microanalysis to identify platinum group minerals

Ronald J. Bakker

Resource Mineralogy
Department of Applied Geosciences and Geophysics
Montan-University Leoben
Austria

bakker@unileoben.ac.at

Abstract

The identification of minerals that occur as tiny and rare phases such as most of the natural platinum group minerals (PGM) is a challenging target. The main reason for that resides in their size (generally less than 10 microns) and mode of occurrence (i.e. polyphasic aggregates) that prevents any XRD structural study. Raman spectroscopy is innovative and complementary methodology with a potential to identify and to better characterize the PGM. The Raman spectra of only a limited number of PGM's are known (about 24), and they are presented in this study. They can be directly used to identify or verify small sized PGE-bearing phases that were detected by reflection microscopy or electron probe analyses. Most PGM's belong to the elements (about 30) and the sulphides (about 90). PGE-bearing oxides and hydroxides are not yet represented by minerals, but abundant spectra are available from physical chemistry, which are also presented in this study. These spectra may be highly valuable for the identification of these phases in nature.

1. Introduction

The platinum group elements (PGE) are mainly present in sulphides, tellurides, arsenides, alloys and oxides, that belong to the following subgroups according to Strunz and Nickel (2001): (01.A) metallic and intermetallic compounds; (02.A) alloys; and (02.B, 02.C, 02.D, 02.E) sulphides with variable metal-sulphur ratio (or selenium, tellurium, arsenic, antimony, and bismuth). The oxides (and hydroxides) of PGE's are only defined as "unnamed" according to IMA, apart from palladinite (PdO), and are mainly formed by desulphurization during hydrothermal events (e.g. Garuti et al. 1997; Uysal et al., 2009; Locmelis et al., 2010). Mineralogical, crystallographical and geochemical properties of these minerals have been described by e.g. Wood (1987), Sassani and Shock (1998), and Cabri, (2002), whereas the geological occurrence and economic importance was elucidated by e.g. Cabri (2002). Platinum group minerals (PGM) are usually associated with chromite, Bi-tellurides, Cu-Fe-sulphides, (Co,Ni)AsS, and hydrous minerals such as amphibole and chlorite.

The detection of PGM's is usually performed with reflection optical microscopy and electron probe by using a variety of analytical techniques, such as EDS and WDS. Occasionally, these analytical techniques may not result in the identification of PGM's due to the relative small size of PGM-grains. The electron probe generally provides only semi-quantitative analyses of small grains due interferences from surrounding minerals. In addition, specific minerals with similar compositions but different structures cannot be identified (polymorphism). This study is focused on the use of Raman spectroscopy, as a

complementary method to electron probe analyses, to identify PGM's. Raman spectroscopy does not require a complex sample preparation because 1. coating and a vacuum are not necessary; 2. polymorphic minerals can be identified, and 3. the size of the measured object can be as small as 1 μm in diameter. There is only few data available of Raman spectra of PGM's (e.g. RRUFF, <http://rruff.info/>), and this study summarizes reported spectra of PGM's and chemical compounds that contain PGE's. In additions, new Raman spectra are measured of a variety of PGM's. These PGM's were first analyzed by an electron probe to produce standard Raman spectra that can be used to identify unknown objects.

2. Raman spectroscopy

Raman spectroscopy is a non destructive and structurally sensitive technique that can be easily used to identify small mineral phases less than 10 microns in size, such as PGM's. Raman spectroscopy uses the inelastic scattering of light to analyse vibrational and rotational modes of molecules (e.g. Turrell and Corset, 1996). The interaction of the vibration modes of molecules and light causes its loss (*Stokes scattering*) and gain of energy (*Anti-Stokes scattering*). The energy-loss process is most probable, and provides, therefore, a more intense signal (Fig. 1). The vibration modes depend on the symmetry of the molecules, and they cause a change in *polarizability*, i.e. a change in the symmetry of electron orbitals. Therefore, the spectrum is a fingerprint of specific bonds in mineral phases. A well-defined incident light beam (laser), with one specific wavenumber (18794.59 cm^{-1}) and enough power (source 100 mW, 1-2 mW at sample surface) to be able to agitate molecules is therefore necessary to obtain useful numbers on the light scattering. A Stokes Raman spectrum is a plot of the intensity of the scattering expressed in wavenumbers relative to the source ($\Delta\nu$ in cm^{-1} , the *Raman shift*), i.e. the changes in wavenumber compared to the incident light (Fig. 1).

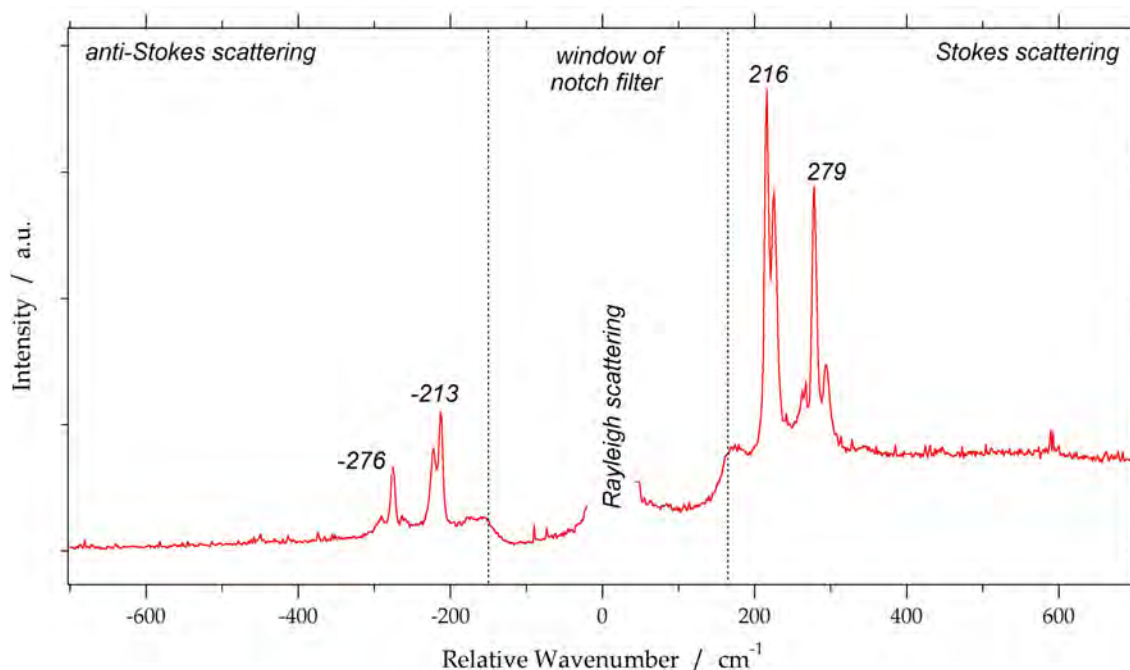


Fig. 1. Raman spectrum of Sperrylite, PtAs₂, illustrating the three types of scattering: Stokes, anti-Stokes, and Rayleigh. The boundaries of the notch filter are illustrated that is used to reduce the intensity of Rayleigh scattering. The relative wavenumbers ($\Delta\nu$) of peak values of Stokes and anti-Stokes scattering are approximately similar with opposite signs.

Raman spectra were collected using a LABRAM (ISA Jobin Yvon) instrument at the Montan-University Leoben (Fig. 2). A frequency-doubled 100 mW Nd-YAG laser with an excitation wavelength of $\lambda = 532.068$ nm was used. The laser power at the sample surface is about 1 to 2 mW. Both notch-filter (532 nm, blocking relative wavenumbers below 170 cm^{-1}) and edge-filter (532 nm, blocking relative wavenumbers below 80 cm^{-1}) were used to suppress Rayleigh scattering and anti-Stokes scattering. Measurements were carried out with an LMPlanFI 100x/0.8 (Olympus) objective lens and they have a spectral resolution of 1.62 cm^{-1} at low $\Delta\nu$ (about 0 cm^{-1}) and of 1.1 cm^{-1} at high $\Delta\nu$ (about 3000 cm^{-1}). Additional neutral filters with variable optical densities were used to decrease the laser power to prevent damage or transformation of the samples. Simultaneously measured Neon emission lines were used for calibration.



Fig. 2. The ISA Jobin Yvon LABRAM (Horiba) laser Raman microprobe, combined with an Olympus BX 40 microscope at the chair of Resource Mineralogy, Montan-University Leoben, Austria.

3. Raman spectra of elements: metals and intermetallic alloys

In general, due to the metallic character of chemical bonds in the subgroups PGE and PGE-metal alloys (01.AF and 01.AG) it is unlikely to obtain well-defined Raman spectra of these minerals. The Raman spectroscopic data bank RRUFF (<http://rruff.info/>) provides only poor spectra of osmium, iridium, palladium, platinum, and isoferroplatine, Pt_3Fe , that cannot be used to identify these mineral phases. Spectra of ruthenium and rhodium are not presented. Garutiite, (Ni, Fe, Ir), does not show discernible Raman bands over the $\Delta\nu$ range of 150 to 2000 cm^{-1} (McDonald et al., 2010). Mernagh and Hoatson (1995) report a Raman spectrum of potarite, PdHg , from the mercury-metal subgroup (01.AD), with a broad main peak at about 340 cm^{-1} and a large *FWHM* ($\approx 50\text{ cm}^{-1}$), with a shoulder-peak at about 362 cm^{-1} .

Synthetic Pd-endmember of atokite, $(\text{Pd,Pt})_3\text{Sn}$, (Vymazalova et al, in press) has a broad band between 400 and 1100 cm^{-1} , which can be assigned to various deconvolved Gaussian-Lorentzian distribution curves (Fig. 3). Deconvolution with 6 distribution curves is determined by the minimum number of best-fit curves that describe accurately the obtained spectrum. The best-fit curves are not associated with specific theoretical vibration and rotation modes of the material, or interference patterns. These curves are centered at about 380 , 465 , 570 , 792 , 984 , and 1091 cm^{-1} , with relative broad *FWHM* varying between 25 and 180 cm^{-1} (Fig. 3). The uncertainty in the centre positions is about 20 cm^{-1} .

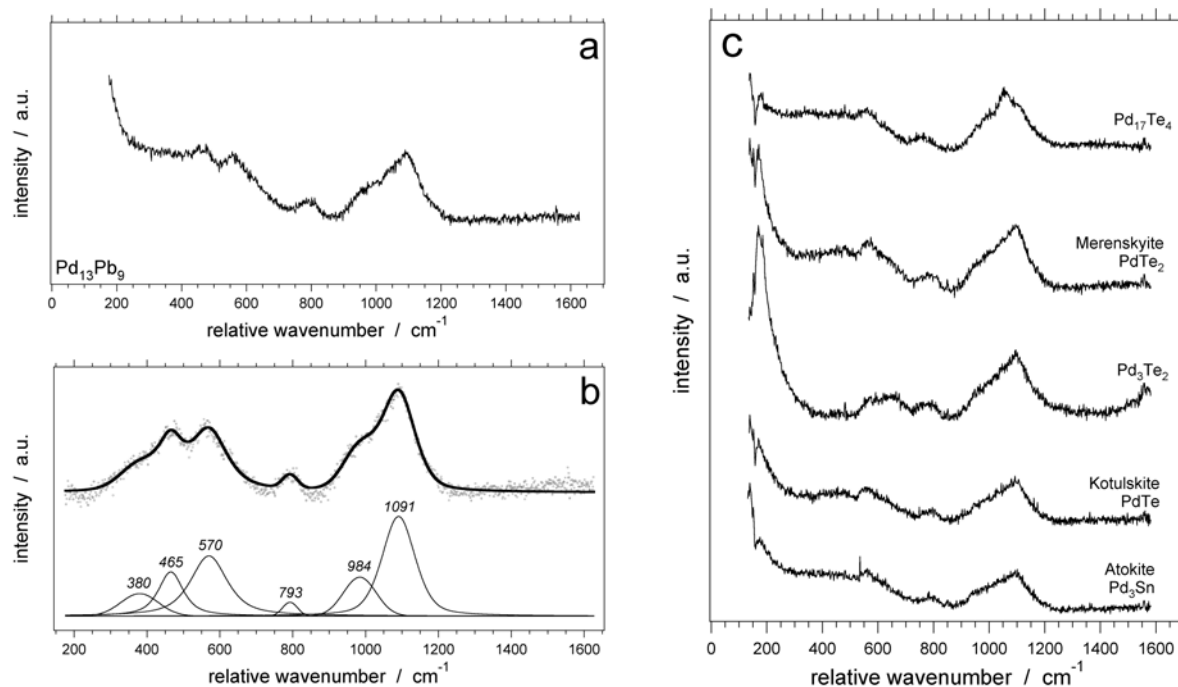


Fig. 3. (a) Raman spectrum of synthetic $\text{Pd}_{13}\text{Pb}_9$; (b) deconvoluted Raman spectrum of this spectrum after background subtraction with 6 best-fit Gaussian-Lorentzian distribution curves, numbers in diagram illustrate centre position of distribution curves. The software Peakfit (2002, version 4.11) was used to deconvolve this spectrum; (c) Comparison of Raman spectra in the binary Pd-Te system and binary Pd-Sn system (after Vymazalova et al., in press).

4. Raman spectra of sulphides: alloys and metalloids with PGE

This mineral subgroup (02.AC) contains abundant PGM's, but the corresponding Raman spectra are rare. RRUFF reports only the spectra of rhodarsenide, $(\text{Rh,Pd})_2\text{As}$, polkanovite, $(\text{Rh,Ni})_{12}\text{As}_7$, and froodite, PdBi_2 , which cannot be used to identify these phases due to the poor quality. The spectra of isomertieite, $\text{Pd}_{11}\text{Sb}_2\text{As}_2$, and stibiopalladinite, Pd_5Sb_2 , were presented by Bakker (2010) and reveal a main peak at 136 cm^{-1} and 108 cm^{-1} , respectively (Fig. 4). In addition, stibiopalladinite contains two minor peaks at 169 cm^{-1} and 187 cm^{-1} .

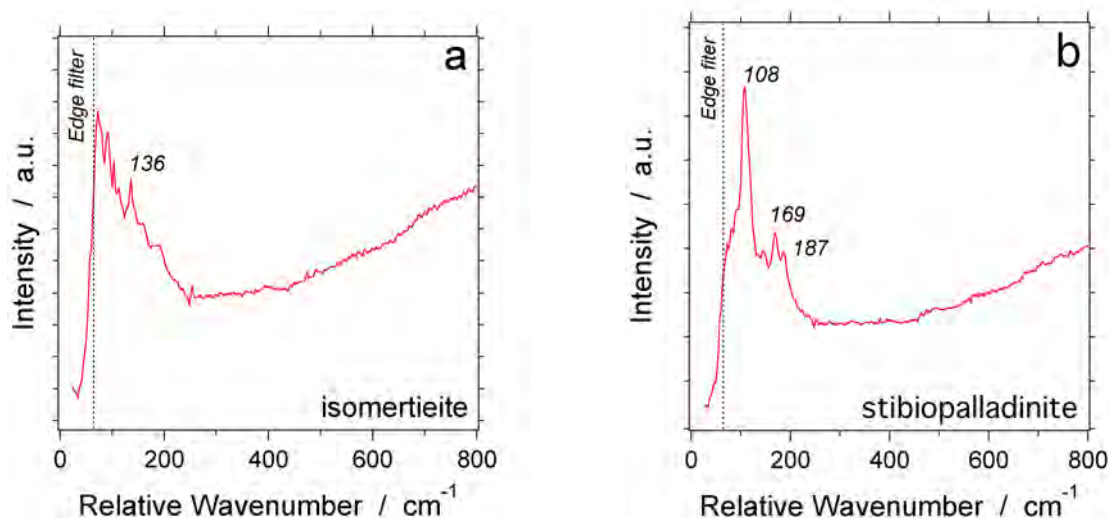


Fig. 4. The Raman spectra of (a) isomertieite, $\text{Pd}_{11}\text{Sb}_2\text{As}_2$, and (b) stibiopalladinite, Pd_5Sb_2 . The relative wavenumber limit of the edge filter is illustrated in both spectra.

5. Raman spectra of sulphides: metal sulphides $M:S > 1:1$ with PGE's

This mineral subgroup (02.BC) contains 15 PGM's, of which Raman spectra have not been reported in RRUFF, apart from the spectra of miassite, $Rh_{17}S_{15}$, and vasilite, $(Pd,Cu)_{16}(S,Te)_7$, but the quality of those spectra do not allow definite identification of these minerals. A high quality spectrum of vasilite was reported by Bakker (2010) that illustrates a major peak at 310 cm^{-1} and various minor peaks at 108, 140, 203, 280 and 388 cm^{-1} (Fig. 5).

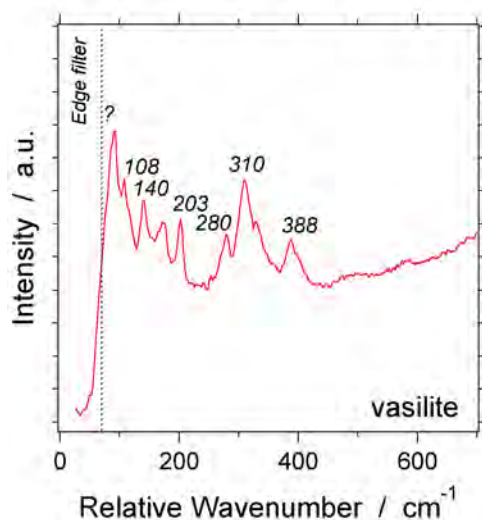


Fig. 5. Raman spectrum of vasilite

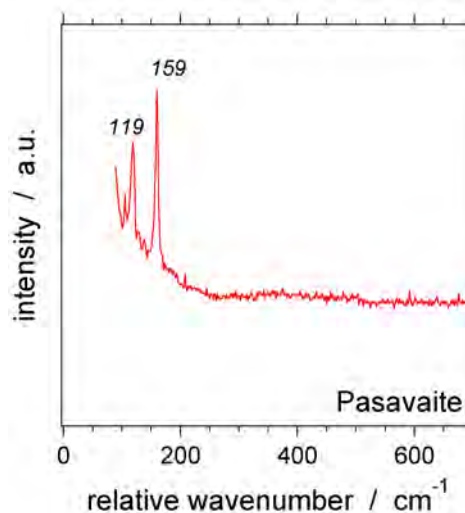


Fig. 6. Raman spectrum of pašavaite

The Shandite-group (02.BE) contains two PGM's of which synthetic pašavaite, $Pd_3Pb_2Te_2$, was analyzed by Vymazalova et al. (in press). The spectrum of pašavaite contains two relative narrow peaks at 119 and 159 cm^{-1} (Fig. 6). The spectrum of kojonenite, $Pd_{7-x}SnTe_2$ ($0.3 \leq x \leq 0.8$), reveals a relative weak and broad Raman band at 197 cm^{-1} (Fig. 7) (Vymazalova et al. (in press)). They also determined the spectrum of synthetic Pd_3Te_2 (Fig. 8), which is not yet defined as a mineral, with a double peak at low relative wavenumbers, 120 and 128 cm^{-1} .

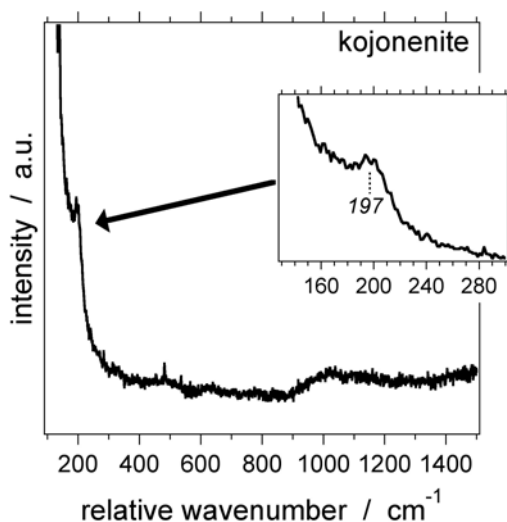


Fig. 7. Raman spectrum of kojonenite

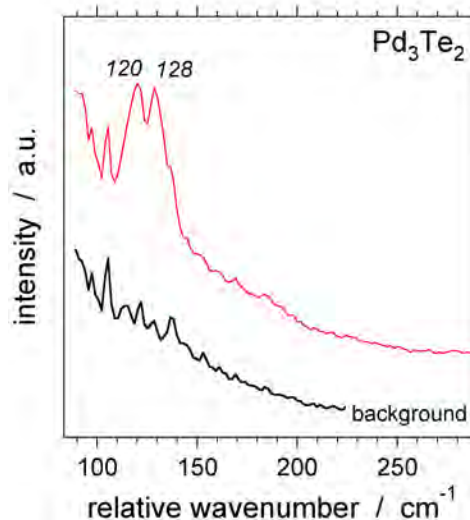
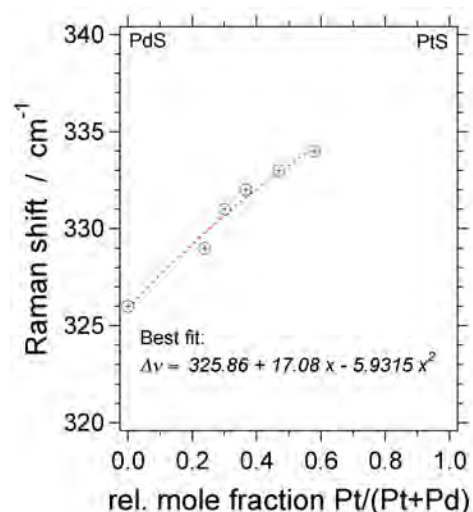


Fig. 8. Raman spectrum of Pd_3Te_2 (red line) compared to the background signal (black line) (Vymazalova et al., in press).

6. Raman spectra of sulphides: metal sulphides M:S = 1:1 with PGE's

The nickel-iron-cobalt-PGE bearing subgroup (02.CC) contains various PGM's. The Raman spectrum of braggite, (Pt,Pd,Ni)S, was presented in various studies (RRUFF; Mernagh and Hoatson, 1995; Merkle et al., 1999; Bakker, 2010), and illustrate an inconsistent variability. The composition of braggite was not identified in some of these studies, which probably causes this variation. Mernagh and Hoatson (1995) described a main peak at 351 cm^{-1} , with shoulder-peaks at 317 cm^{-1} and 379 cm^{-1} for a braggite with unknown composition. Merkle et al. (1999) analysed synthetic braggite with variable Pt-Pd contents and low Ni concentration. The main peak shifts to higher wavenumbers with increasing Pt content, from 326 cm^{-1} (PdS) to 334 cm^{-1} ($\text{Pt}_{0.55}\text{Pd}_{0.40}\text{Ni}_{0.04}\text{S}$) (Fig. 9). The Raman signal contains one broad band between 350 and 400 cm^{-1} . These spectra are completely different from the natural braggite analysed by Mernagh and Hoatson (1995), which probably contained a different percentage of Ni. The Raman spectrum of braggite measured by Bakker (2010) is illustrated in Fig. 10, and is characterized by at least four peaks of equal intensity: 111 cm^{-1} , 330 cm^{-1} , 360 cm^{-1} and 378 cm^{-1} , which approximately corresponds to the broad band between 300 and 400 cm^{-1}



illustrated by Mernagh and Hoatson (1995). Cooperite, PtS, reveals a different pattern in Raman spectra, and is characterized by a broad main peak at about 332 cm^{-1} , with shoulder-peaks at 319 cm^{-1} , 347 cm^{-1} , and 365 cm^{-1} (Mernagh and Hoatson, 1995). RRUFF presents a similar spectrum with the main peak at 330 cm^{-1} and a minor peak at 354 cm^{-1} (Fig. 11). It should be noted that the RRUFF spectrum is erroneously indicated as a braggite spectrum, with the composition PtS (c.f. Verryyn and Merkle, 2000).

Fig.9. Shift in $\Delta\nu$ of the main peak of synthetic braggite according to Merkle et al. (1999), with a best-fit equation for its compositional dependency.

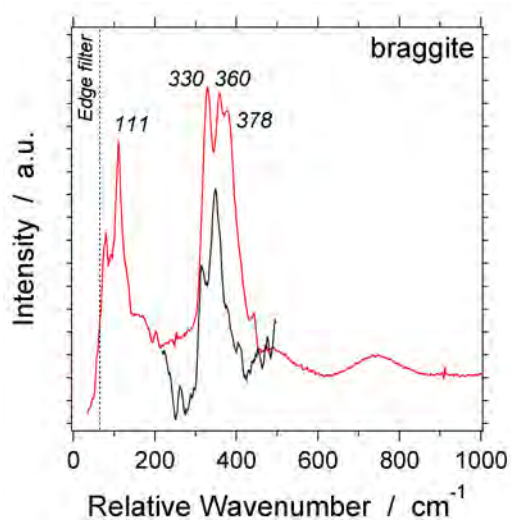


Fig. 10. Raman spectra of braggite from Bakker (2010), red line, and Mernagh and Hoatson (1995), black line.

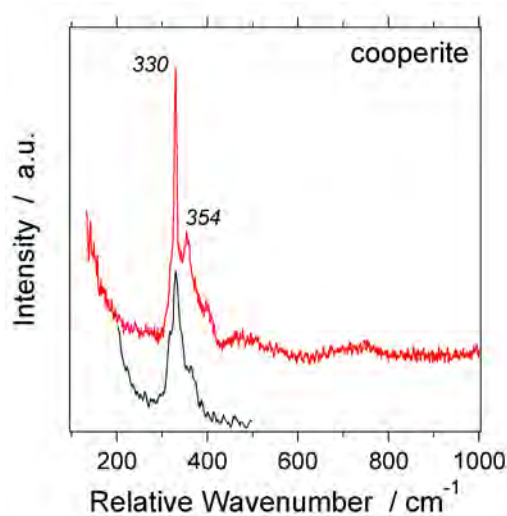


Fig. 11. Raman spectra of cooperite from RRUFF, red line, and Mernagh and Hoatson (1995), black line.

Sobolevskite, PdBi, does not show discernible Raman bands over the $\Delta\nu$ range of 150 to 2000 cm^{-1} (Bakker, 2010). Synthetic Te-rich kotelskite (PdTe) was described by Vymazalova et al. (in press) and reveal a similar weak spectrum as synthetic atokite in the range of 300 to 1600 cm^{-1} (Fig. 3). However, they detected a Raman band at low relative wavenumbers, about 97 cm^{-1} (Fig. 12). The Raman spectra of other PGM's in this subgroup were not investigated.

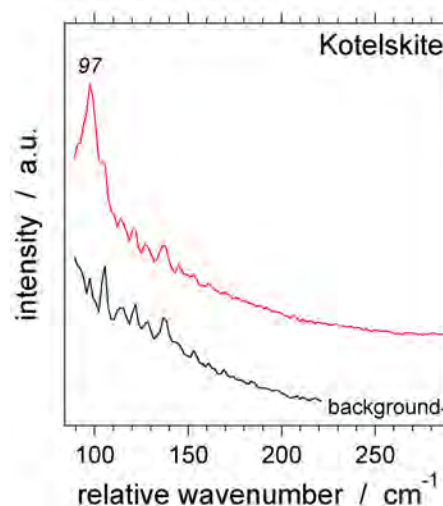


Fig. 12. Raman spectrum of kotelskite (red line) compared to the background signal (black line).

7. Raman spectra of sulphides: metal sulphides M:S = 3:4 and 2:3 with PGE's

This mineral group (02.DA and 02.DB) contains seven PGM's of which only malanite, CuPt_2S_4 , and bowieite, Rh_2S_3 , are reported by RRUFF, but the quality of those spectra does not allow definite identification of these minerals. Two spectra of kashinite, $(\text{Ir,Rh})_2\text{S}_3$, were reported by Bakker (2010) with a major peak at 298 cm^{-1} or a double peak at 290 and 311 cm^{-1} (Fig. 13), and minor peak at 368 or 389 cm^{-1} .

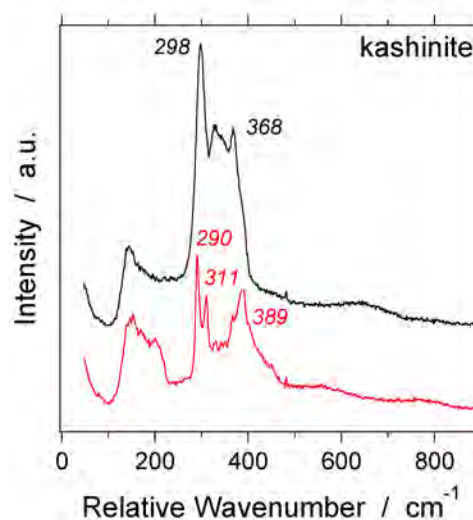


Fig. 13. Raman spectra of kashinite (Bakker, 2010).

8. Raman spectra of sulphides: metal sulphides M:S = 1:2 with PGE's

The melonite subgroup (02.EA.20), pyrite subgroup (02.EB.05), and the gersdorffite subgroup (02.EB.25) contain numerous PGM's.

Melonite subgroup

Synthetic merenskyite, PdTe_2 , was described by Vymazalova et al. (in press) and reveals a similar spectrum as synthetic atokite (Fig. 3). At low relative wavenumbers, merenskyite has a clear Raman band at 132 cm^{-1} (Fig. 14). The Raman spectrum of moncheite, $(\text{Pt,Pd})(\text{Te,Bi})_2$, has a main peak at 115 cm^{-1} and a minor band at 155 cm^{-1} (Mernagh and Hoatson, 1995) (Fig. 15). This spectrum is similar to that of synthetic pašavaite (c.f. Fig. 6).

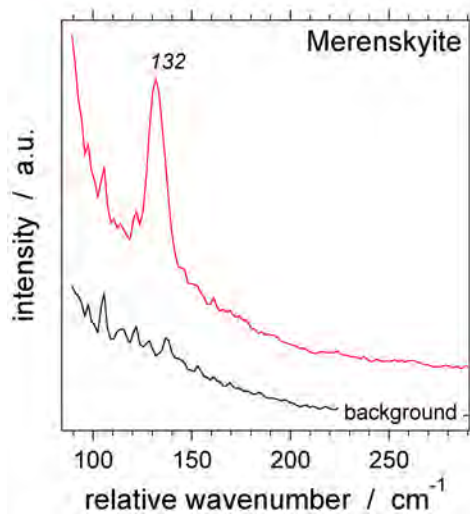


Fig. 14. Raman spectra of merenskyite (red line) compared to background signal (black line)..

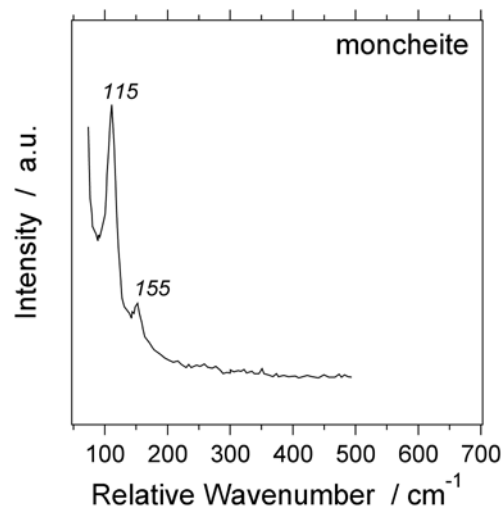


Fig. 15. Raman spectrum of moncheite.

Pyrite subgroup

Insizwaite, $\text{Pt}(\text{Bi},\text{Sb})_2$, has narrow Raman bands at relatively low wavenumbers: 96, 114 and 126 cm^{-1} (Bakker, 2010) (Fig. 16). The low quality spectrum reported by RRUFF does not include this range of wavenumbers, illustrating the importance of analysing relatively low relative wavenumbers of PGM's, by the use of edge-filters. Müller and Lutz (1991) report the spectra of RuTe_2 and OsTe_2 with the major Raman band at 179 and 175 cm^{-1} , respectively. These tellurides have a pyrite-type structure, but are not yet defined as minerals.

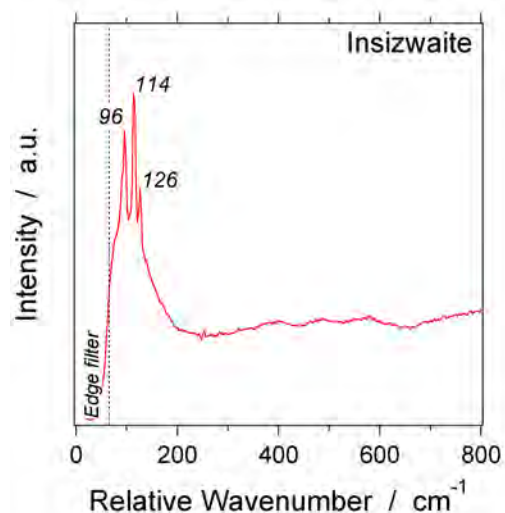


Fig. 16. Raman spectrum of insizwaite (Bakker, 2010)

A complete solid solution is possible between laurite, RuS_2 , and erlichmanite, OsS_2 , with considerable substitution of other PGE's (e.g. Bowles et al., 1983). Consequently, a complete series of Raman spectra can be obtained to illustrate the Raman shift of the main peak with relative Ru/Os ratio (e.g. Stingl et al., 1992) (Fig. 17). Hwang et al. (1994) illustrate the Raman shift of laurite due to the substitution with Fe. The main broad band of $\text{Fe}_{0.5}\text{Ru}_{0.5}\text{S}_2$ was estimated at 377 cm^{-1} .

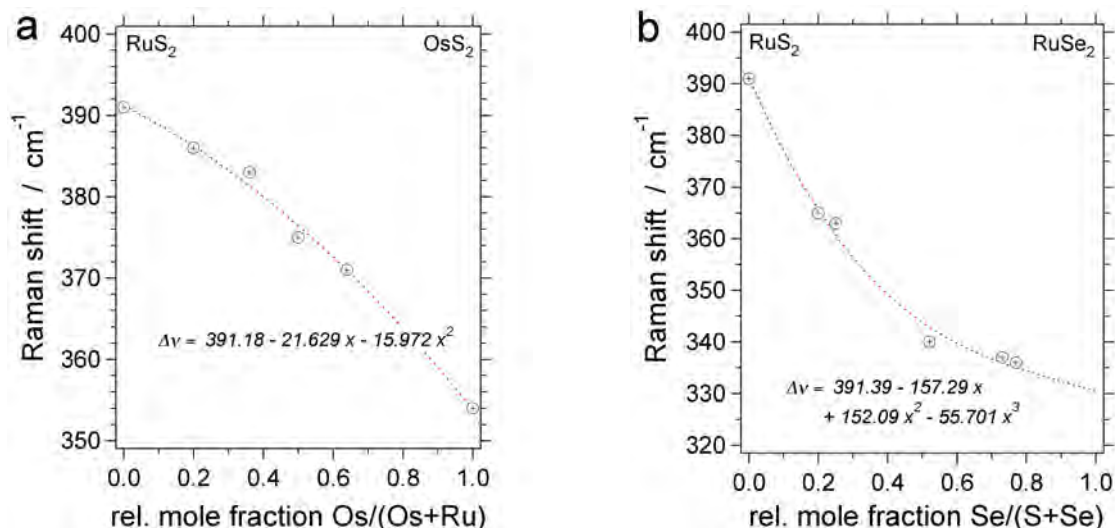


Fig. 17. Shift of the main Raman band of laurite as a function of Os/Ru ratio (a) and Se/S ratio (b) according to Stingl et al. (1992). Best-fit equations are given in both diagrams, which can be used to perform quasi-chemical analyses based on Raman spectroscopy.

The Raman spectra of natural laurite (Fig. 18) do not correspond to the theoretical values illustrated by Stingl et al., 1992). Laurite contains a well-defined main peak at about 356.5 cm^{-1} (RRUFF), and may vary between 351 , 352 , and 364 cm^{-1} according to Bakker (2010). This Raman band has a shoulder at about 395 cm^{-1} . The variation is most probably a result of various concentrations of Os in laurite.

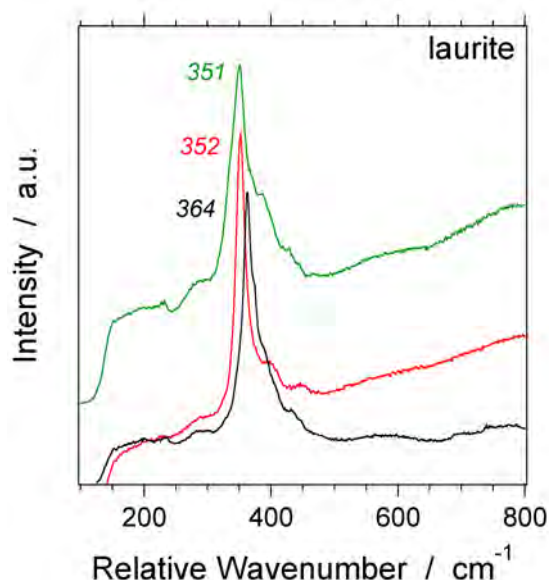


Fig. 18. Raman spectra of three different natural laurite crystals (Bakker, 2010).

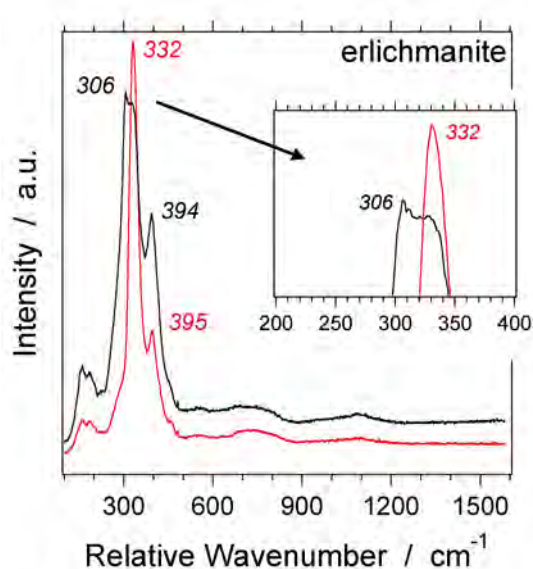


Fig. 19. Raman spectra of the same erlichmanite crystal in two different orientations relative to the polarization direction of the laser source (Bakker, 2010).

Erlichmanite has a similar spectrum, but the main Raman band is shifted to lower wavenumbers: $306\text{-}332 \text{ cm}^{-1}$ (Fig. 19). Due to the anisotropic properties of an erlichmanite crystal, the Raman intensities of individual peaks may vary in intensity, dependent on the crystal orientation in relation to the polarization direction of the laser source. The peak at 306

cm^{-1} is only a minor shoulder in specific orientations, whereas in other orientations this peak may exceed the intensity of the major peak at 332 cm^{-1} (Fig. 19). The spectrum in RRUFF reveals a well-defined Raman band at 330 cm^{-1} , but the spectrum is highly affected by interferences with other unknown mineral phases.

Sperrylite, PtAs_2 , has its main Raman band at 216 cm^{-1} (Mernagh and Hoatson, 1995). This peak was confirmed by Bakker (2010), who illustrated in detail additional peaks (Fig. 20: two main peaks at 216 and $279\text{-}280 \text{ cm}^{-1}$, minor peaks appear at 226 and $293\text{-}297 \text{ cm}^{-1}$, with variable intensity dependent on the orientation of the crystal).

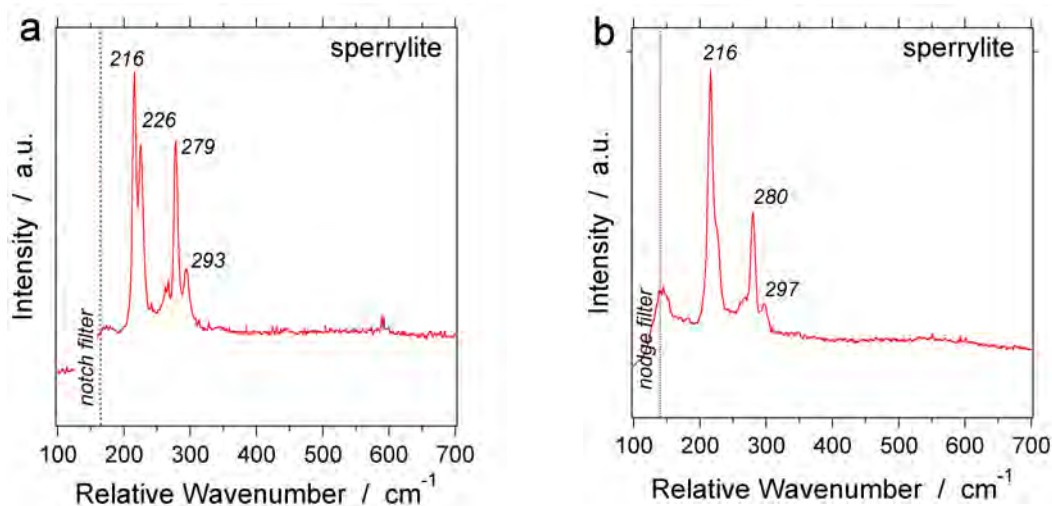


Fig. 20. Two Raman spectra of sperrylite (a, b) according to Bakker (2010).

Gersdorffite subgroup

Hollingworthite, $(\text{Rh,Pt,Pd})\text{AsS}$, irarsite, $(\text{Ir,Ru,Rh,Pt})\text{AsS}$, and platarsite, $(\text{Pt,Rh,Ru})\text{AsS}$, are similar sulfarsenide minerals, which are relatively enriched in Rh, Ir, and Pt, respectively, that can be distinguished by Raman spectroscopy (Fig. 21, 22, and 23, respectively).

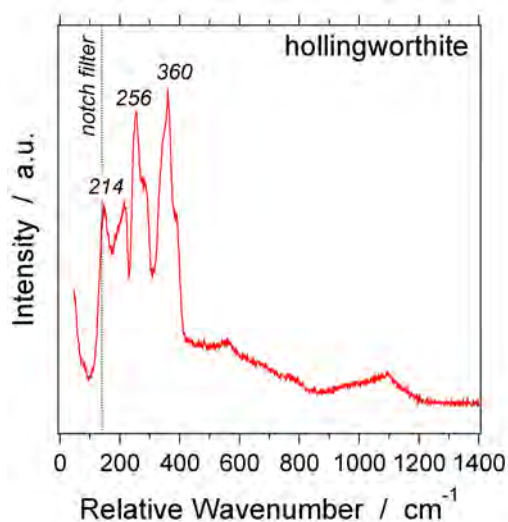


Fig. 21. Raman spectrum of hollingworthite (Bakker, 2010).

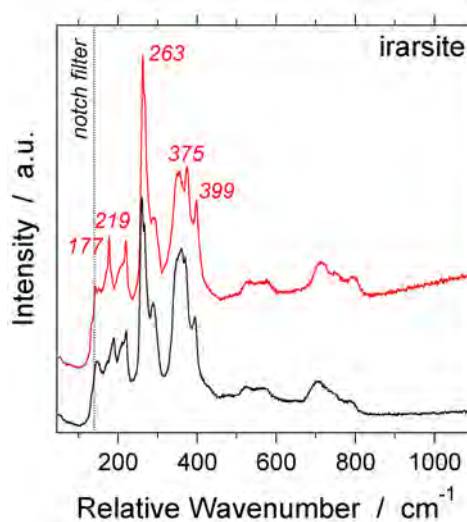


Fig. 22. Raman spectra of the same irarsite crystal in two different orientations (Bakker, 2010).

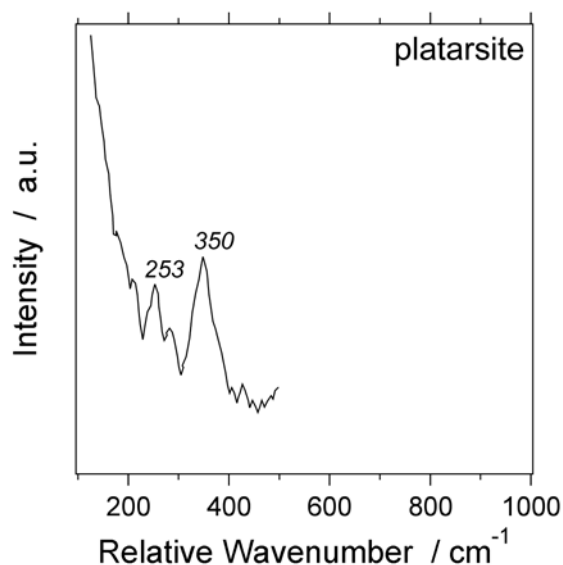


Fig. 23. Raman spectrum of platarsite (Mernagh and Hoatson, 1995).

The Raman spectra in this group are mainly defined by two bands: 375-360-350 cm⁻¹ and 263-256-253 cm⁻¹, which can be used to identify irarsite, hollingworthite, or platarsite, respectively (Table 1). RRUFF databank does not provide spectra of these PGM's, but reveals only one spectrum of tolovkite, IrSbS, with a main peak at approximately 350 cm⁻¹ and a shoulder-peak at 370 cm⁻¹ (Fig. 24).

Table 1. Comparison of the main Raman bands of irarsite, hollingworthite and platarsite (wavenumbers, cm⁻¹).

irarsite	177	219	263	375	399
hollingworthite		214	256	360	
platarsite			253	350	

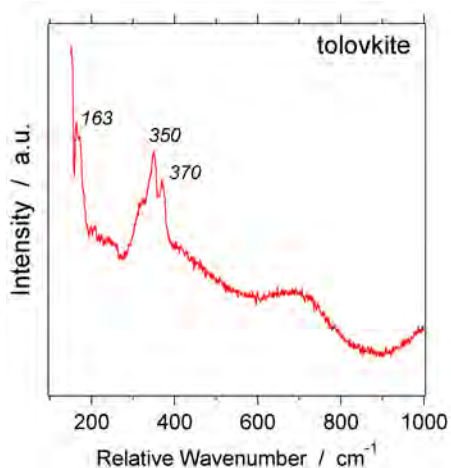


Fig. 24. Raman spectrum of tolovkite (RRUFF).

9. Raman spectra of oxides and hydroxides with PGE's

Palladinite, PdO, is one of the few PGM's that are confirmed to occur in nature. Abundant PGE-bearing oxides and hydroxides are still known as "unnamed" according to IMA, such as Pd(OH), PdO·3H₂O, (Bi₂O₃,Pd), Pd₉PbO₁₀, Pd₅Sb₂O₄, Pd₃(Sb,Bi)₂O₄, (Ir,Rh)O(OH)·H₂O, IrO₂, (Ru,Os,Ir,Fe,Ni,Cu)₁₋₂O₂₋₃, (Ru,Fe)₂O₃. RRUFF does not provide any Raman spectra of

these minerals. Synthetic samples, including thin-film samples and microcrystalline samples of various PGE-oxides were analysed by e.g. Weber et al. (1988) and Graham et al. (1991). The Raman spectrum of synthetic palladinite reveals two main peaks at 445 and 650 cm^{-1} (Weber et al., 1988) (Fig.25). These peaks are shifted to 438 and 657 cm^{-1} for synthetic PtO (Fig. 26) that reveal larger *FWHM*'s, and illustrate interference with amorphous PtO (Graham et al., 1991).

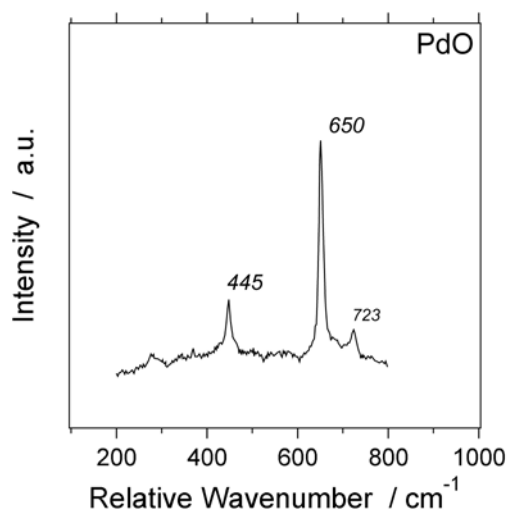


Fig. 25. Raman spectrum of synthetic palladinite.

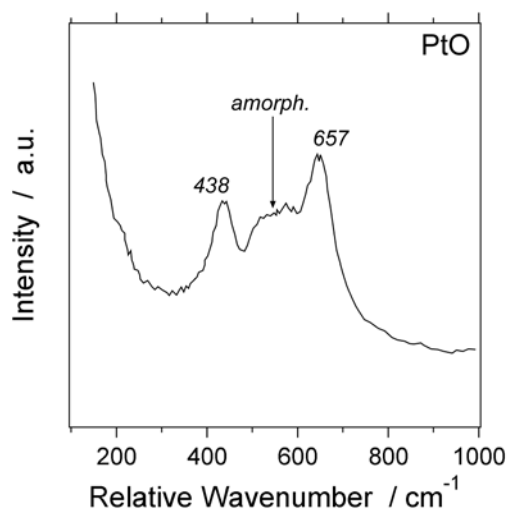


Fig. 26. Raman spectrum of synthetic PtO, partly amorphous.

The multiple oxidation states of Pt can be visualized by Raman spectroscopy, through comparison with the spectra of PtO, PtO₂, Pt₃O₄ and Pt₅O₆ (Graham et al., 1991) (Figs. 26, 27, 28, 29). PtO₂ can crystallize in a low temperature modification (α -PtO₂) and a high temperature modification (β -PtO₂), similar to the modifications of TiO₂ (rutile and anatase), and reveal distinct Raman spectra (Fig. 27). The Pt₃O₄ spectrum illustrates similarities with the spectra of the spinel group (e.g. magnetite), i.e. with a relative large *FWHM* for the main band at 708 cm^{-1} (Fig. 28). Pt₅O₆ reveals two major peaks at 527 and 670 cm^{-1} with shoulder-peaks at 509 and 642 cm^{-1} (Fig. 29.). These examples illustrate that Raman spectroscopy is a complementary analytical technique to electron probe analyses, to specify the crystallinity and oxidation state of multi-valence elements in PGM's.

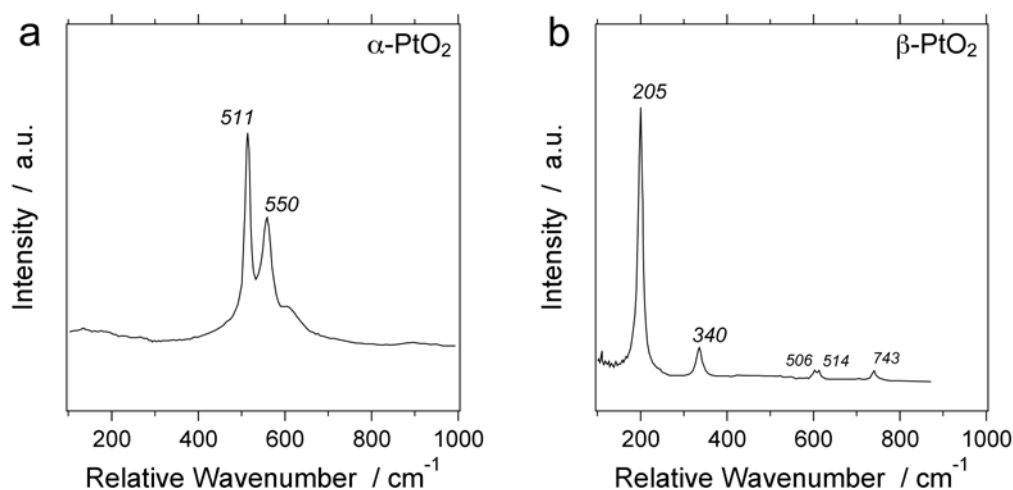


Fig. 27. Raman spectra of the modifications of PtO₂ (a, b).

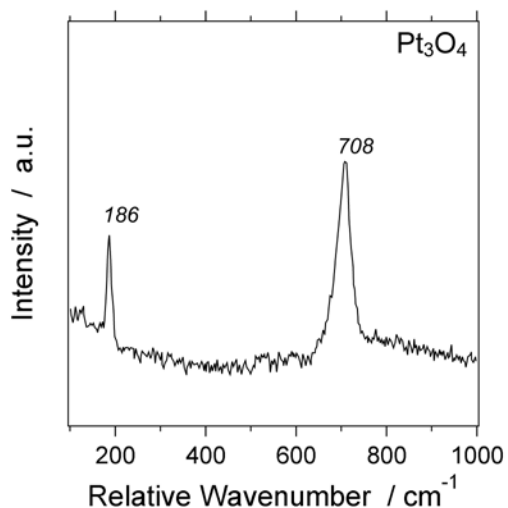


Fig. 28. Raman spectrum of synthetic Pt₃O₄.

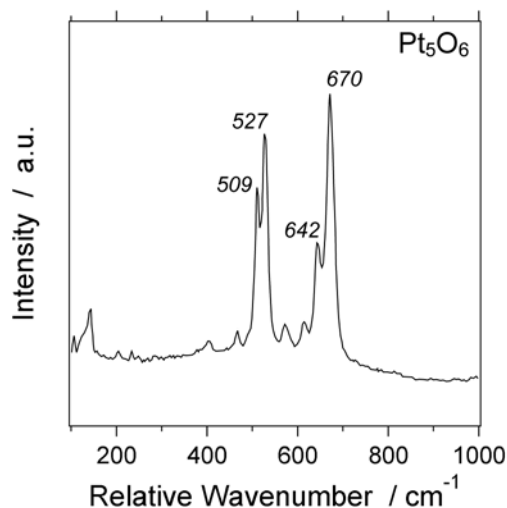


Fig. 29. Raman spectrum of synthetic Pt₅O₆.

Synthetic Rh₂O₃ has two major Raman bands at 277 and 426 cm⁻¹, and two minor peaks at 572 and 614 cm⁻¹ (Weber et al., 1988) (Fig. 30). Synthetic OsO₄ has a major band at about 964 cm⁻¹, and several minor bands at 335 and 954 cm⁻¹ (e.g. McDowell and Goldblatt, 1971).

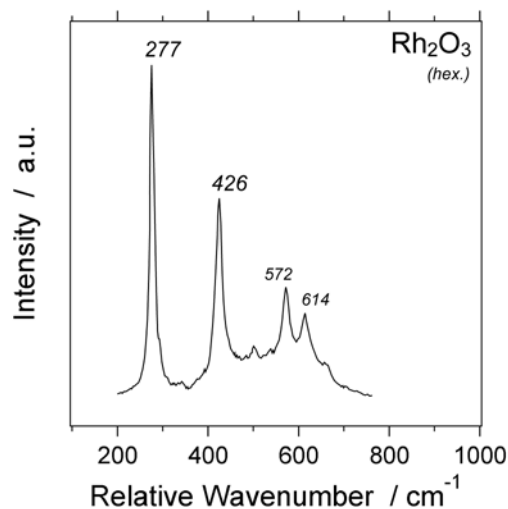


Fig. 30. Raman spectrum of Rh₂O₃, hexagonal.

The Pt and Pd oxides may combine with transition metals, such as Co, Mn and Cd, or with other PGE's to form associated oxides with specific Raman spectra (Figs. 31, 32 and 33).

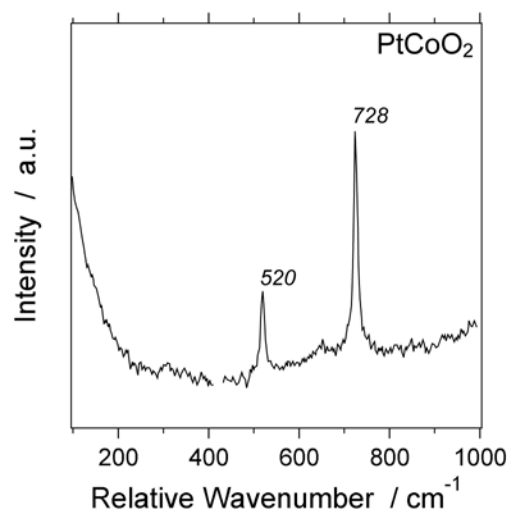


Fig. 31. Raman spectrum of synthetic PtCoO₂ (Graham et al., 1991).

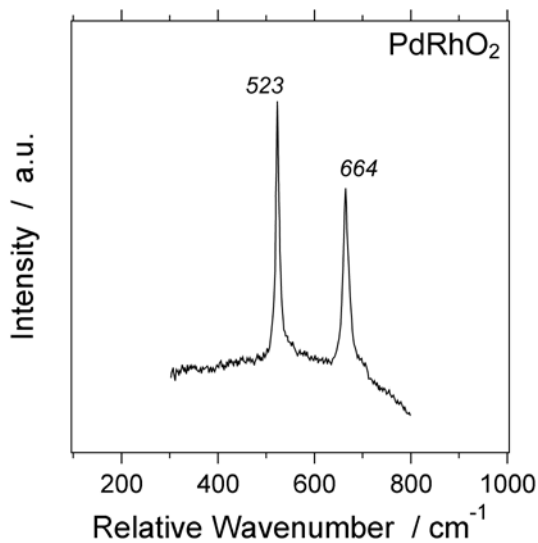


Fig. 32. Raman spectrum of synthetic Pt_5O_6 (Weber et al. 1988)

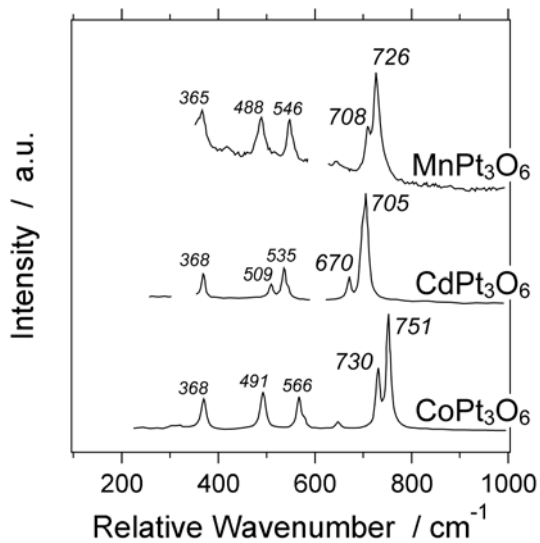


Fig. 33. Raman spectra of MnPt_3O_6 , CdPt_3O_6 and CoPt_3O_6 (Graham et al., 1991).

Renard et al. (2006) describes the Raman spectrum of $\text{Sr}_4\text{PbPtO}_{11}$, PbPt_2O_4 , Sr_4PtO_6 , and $\text{Bi}_{1.6}\text{Pb}_{0.4}\text{PtO}_4$, with major peaks at 594 cm^{-1} , 526 cm^{-1} , 519 cm^{-1} , and 246 cm^{-1} , respectively (Fig. 34).

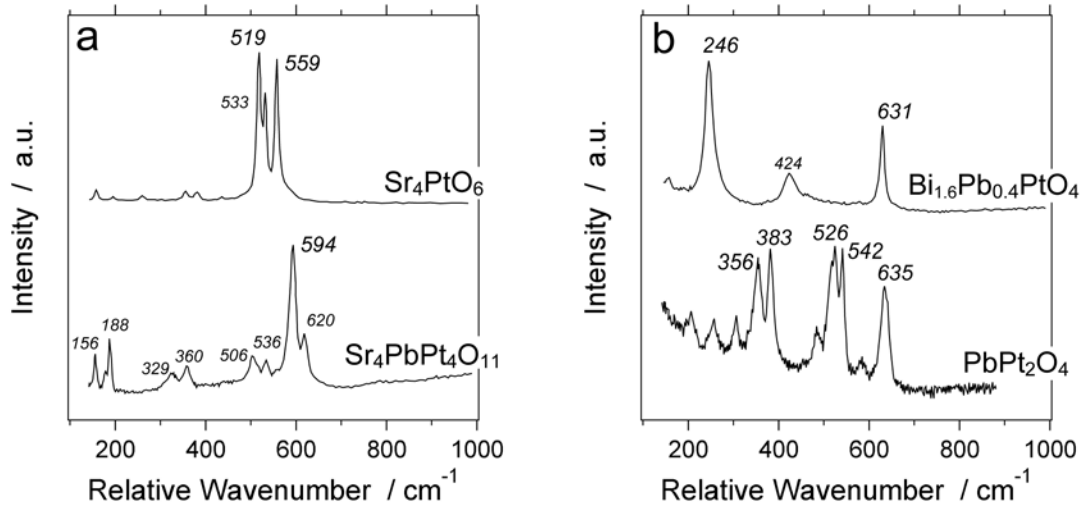


Fig. 34. Raman spectra of (a) Sr_4PtO_6 and $\text{Sr}_4\text{PbPtO}_{11}$; (b) $\text{Bi}_{1.6}\text{Pb}_{0.4}\text{PtO}_4$ and PbPt_2O_4 .

References

- Bakker RJ (2010) Raman Spectroscopy: application to platinum-group minerals. Short Course: Mineralogy, geochemistry, and ore deposits of platinum group elements (Mogessie et al. eds.), 20th General Meeting of IMA, Budapest.
- Bowles JFW, Atkin D, Lambert JLM (1983) The chemistry, reflectance, and cell size of the erlichmanite (OsS_2) - laurite (RuS_2) series. Mineral. Mag., vol. 47, 465-471.
- Cabri LJ (2002) The geology, geochemistry, mineralogy and mineral beneficiation of platinum-group elements. CIM Special Volume 54.

- Garuti G, Zaccarini F, Cabella R, Fershtater G (1997) Occurrence of unknown Ru-Os-Ir-Fe oxides in the chromitites of the Nurali Ultramafic Complex, Southern Urals, Russia. *Can. Mineral.*, vol. 35, 1431-1439.
- Graham GW, Weber WH, McBride JR, Peters CR (1991) Raman investigation of simple and complex oxides of platinum. *J. Raman Spec.*, vol. 22, 1-9.
- Hwang S-T, Lee M-C, Tsay M-Y, Huang Y-S (1994) Raman scattering of $\text{Fe}_x\text{Ru}_{1-x}\text{S}_2$ mixed crystals. *Jpn. J. Appl. Phys.*, vol. 33, 6203-6206.
- Locmelis M, Melcher F, Oberthür T (2010) Platinum-group element distribution in the oxidized Main Sulfide Zone, Great Dyle, Ziwababwe. *Miner. Deposita*, vol. 45, 93-109.
- McDonald AM, Proenza JA, Zaccarini F, Rudashevsky NS, Cabri LJ, Stanley CJ, Rudashevsky VN, Melgarejo JC, Lewis JF, Longo F, Bakker RJ (2010) Garutiite, (Ni,Fe,Ir) , a new hexagonal polymorph of native Ni from Loma Peguerra, Dominican Republic. *Eur. J. Mineral.*, vol. 22, 293-304.
- McDowell RS, Goldblatt M (1971) Vibrational spectrum and force field of osmium tetroxide. *Inorg. Chem.*, vol. 10, 625-630.
- Merkle RKW, Pikel R, Verryin SMC, de Waal D (1999) Raman spectra of synthetic 'braggite', $(\text{Pd,Pt,Ni})\text{S}$. *Mineral. Mag.*, vol 63, 363-367.
- Mernagh TP, Hoatson DM (1995) A laser-Raman microprobe study of platinum-group minerals from the Munni Munni layered intrusion, West Pilbara Block, Western Australia. *Can. Mineral.*, vol. 33, 409-417.
- Müller B, Lutz HD (1991) Raman spectra of MnSe_2 , MnTe_2 , RuTe_2 , and OsTe_2 . *Solid State Comm.*, vol. 78, 469-471.
- Renard C, Roussel P, Rubbens A, Daviero-Minaud S, Abraham F (2006) $\text{Sr}_4\text{PbPt}_4\text{O}_{11}$, the first platinum oxide containing Pt_2^{6+} ions. *J Solid State Chem.*, vol. 179, 2101-2110.
- Stingl T, Muller B, Lutz HD (1992) Pyrite-type $\text{RuS}_{2-2x}\text{Se}_{2x}$ and $\text{Ru}_{1-x}\text{Os}_x\text{S}_2$ solid solutions - X-ray structure determinations and Raman-spectra. *J. Alloys and Compounds*, vol. 184, 275-284.
- Strunz H, Nickel EH (2001) *Strunz Mineralogical Tables*. Ninth Edition, E. Schweizerbart'sche Verlagbuchhandlung, Stuttgart, pp. 870.
- Turrell G, Corset J (1996) *Raman Microscopy, Developments and Applications*. Elsevier Academic Press, Amsterdam, pp. 463.
- Uysal I, Zaccarini F, Sadiklar MB, Bernhardt H-J, Bigi S, Garuti G (2009) Occurrence of rare Ru-Fe-Os-Ir-oxide and associated platinum-group minerals (PGM) in the chromitite of Mugla ophiolite, SW Turkey. *N. Jb. Miner. Abh.*, vol. 185/3, 323-333.
- Verryin SMC, Merkle RKW (2000) Synthetic "cooperite", "braggite", and "vysotskite" in the system PtS-PdS-NiS at 1100 °C, 1000 °C, and 900 °C. *Mineral. Petrol.*, vol. 8, 63-73.
- Vymazalova A, Zaccarini F, Bakker RJ (in press) Raman spectroscopy investigation on synthetic platinum group minerals (PGM) in the ternary systems Pd-Sn-Te and Pd-Pb-Te . *Eur. J. Mineral.*
- Weber WH, Baird RJ, Graham GW (1988) Raman investigation of palladium oxide, rhodium sesquioxide and palladium rhodium oxide. *J. Raman Sep.*, vol. 19, 239-244.
- Wood SC (1987) Thermodynamic calculations of the volatile of the platinum group elements (PGE): the PGE content of fluids at magmatic temperatures. *Geochim. Cosmochim. Acta*, vol. 51, 3041-3050.